Acoustic emission-based monitoring of fatigue damage in CFRP-CFRP adhesively bonded joints

M Carboni and A Bernasconi

Acoustic Emission Based Monitoring of Fatigue Damage in CFRP-CFRP Adhesive Bonded Joints

Michele Carboni[1][0000-0003-0828-9067] and Andrea Bernasconi[1][0000-0002-8611-4134]

[1] Dept. Mechanical Engineering, Politecnico di Milano, Milano, Italy

Abstract. Adhesive bonded joints are more and more applied in modern structures. However, manufacturing defects and particularly harsh operative conditions might cause local de-bonding and catastrophic failures. Structural Health Monitoring and Non-destructive Testing procedures are, then, needed for evaluating the in-service structural integrity of adhesive bonded joints.

In this research, an adhesive bonded single lap joint, whose both adherends are manufactured using a carbon fiber reinforced polymer composite, is subjected to constant amplitude fatigue loading. During such a test, the integrity and damage condition of the joint is continuously monitored by acoustic emission, while the test itself is periodically interrupted in order to apply micro-computed tomography to the specimen, with the aim to investigate the real features of the developing fatigue damage.

Results show that monitoring by acoustic emission, after suitable elaboration and filtering my means of pattern recognition algorithms, allows identifying and characterizing effectively the development of fatigue damage in adhesive bonded joints.
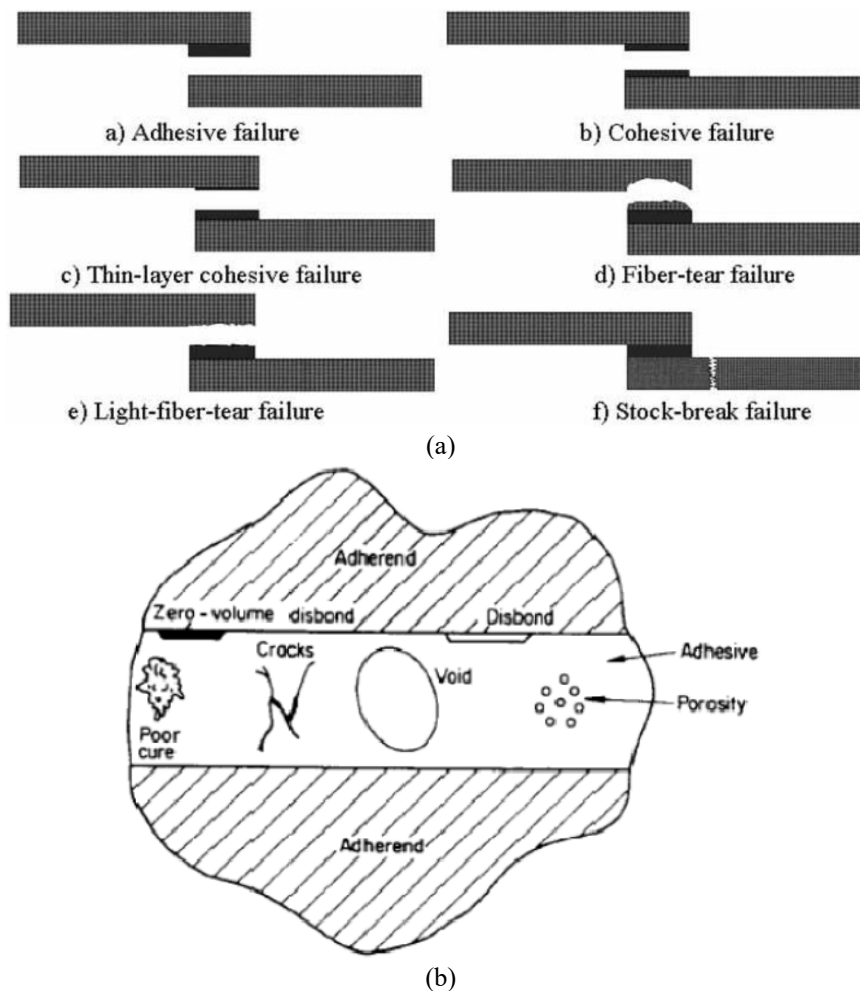
Keywords: CFRP-CFRP adhesive bonded joints, fatigue, acoustic emission, micro computed tomography.

1   Introduction

Adhesive bonding is a solid-state mechanical joining technique where a suitable fluid adhesive, typically a polymeric resin, is inserted between the surfaces of two adherends and, after solidification/polymerization, joins them permanently [1]. In the last years, the adoption of structural adhesive bonded joints has increased, with respect to other more traditional mechanical joining techniques, due to their lighter weight and overall lower manufacturing cost. Other advantages consist in a high stiffness, the possibility to join dissimilar materials, a better stress distribution, a good performance against fatigue loading and a good performance against corrosion (but not in every case). On the other hand, the main drawbacks of adhesive bonded joints consist in the permanent layout, the onset of residual stresses due to manufacturing, the degradation over time due to environmental effects and an inherent difficulty to apply nondestructive testing (NDT) inspections.

The application of adhesive bonding is particularly effective and widespread in the case of composite adherends, especially considering the increasing use of this kind of

2

material in numerous industrial and civil fields. On the other hand, in real applications, adhesive bonding introduces more critical issues for structural integrity because, with respect to traditional joints, multiple and complex failure modes are observed. From this point of view, in the present research, single lap joints between adherends made of "carbon fiber reinforced polymer" (CFRP) are considered and Fig. 1a [1] shows the typical failure modes of this kind of joint. It is worth adding that such failure modes are classified in relevant standards [2] and it is possible to expect that, under some conditions, damage can initiate in the adhesive or in the adherends and, then, propagate into the different components of the joint with a complex behavior.

a) Adhesive failure   b) Cohesive failure

c) Thin-layer cohesive failure   d) Fiber-tear failure

e) Light-fiber-tear failure   f) Stock-break failure

(a)

(b)

Fig. 1. (a) Possible failure modes of a single lap adhesive bonded joint between CFRP adherends [1]. (b) Common defects of the adhesive layer [1].

A primary role, in the competition between the different failure modes, is taken by the typical manufacturing defects originating within the adhesive or at the interface between the adhesive and the adherends. Fig. 1b [1] shows the main cases: the presence of such inhomogeneities and discontinuities in adhesive bonded joints requires, then, the application of maintenance, inspection and monitoring procedures able to guarantee the needed in-service reliability [3]-[5]. Many research studies are available, in the literature, on non-destructive testing (NDT) and structural health monitoring (SHM) of adhesive bonded joints. Summarizing, the most used NDT methods are [4]: visual testing, infrared thermography, ultrasonic testing, radiography and computed tomography (CT). On the other hand, the paradigm is recently shifting towards SHM, because it does not require service interruptions and allows a reduction of maintenance costs of components and systems up to 30% [5]. Today, the most widespread SHM methods applied to adhesive bonded joints are [5] acoustic emission (AE), strain measurement by strain gages or optical fibers and ultrasonic guided waves.

In order to deepen the feasibility of a SHM approach to adhesive bonded joints, the present research analyzes the case of a single lap CFRP-CFRP adhesive bonded joint subjected to fatigue loading, while its damage condition is inspected by visual testing (VT) and x-ray μCT [6], at suitable interruptions of the test, and continuously monitored by AE [7].

2   Experimental set-up

A single lap CFRP-CFRP adhesive bonded joint (Fig. 2a) was fatigue tested. The single adherend has a total thickness equal to 5.3 mm and is composed of 0.66 mm thick laminas arranged as [+45/0$_2$/+45]s. A Scotch Weld 9323 B/A epoxy resin bonds the adherends composing the specimen and the length of the bonded part is equal to 25.4 mm (the total length of the specimen is 285 mm). A uniform adhesive thickness is obtained using 0.2 mm diameter glass spheres as spacers.

The specimen was fatigue tested, under load-controlled conditions, by a uni-axial MTS 810 servo-hydraulic testing machine having maximum capacity equal to 100 kN. The applied cyclic load was characterized by an amplitude of 2 kN and a load ratio equal to 0.05. Particularly, the load level was set on the base of previous fatigue tests carried out on similar joints [8]-[9] and chosen because able to guarantee an average fatigue strength of about 500.000 cycles. In order to focalize the analysis on the first stages of damage development, VT and μCT inspections were carried out at 0 fatigue cycles, at a first interruption of the test after 49100 fatigue cycles and at the forced end of the test (without failure of the specimen) after 109000 fatigue cycles.

VT inspections were carried out on the flanks of the specimen (Fig. 2b) in order to evaluate the location and size of the surface cracks developing from the edges of the overlapped region. A high magnification Dino-Lite digital microscope, together with a Bosch GLI DeciLed LED light, was used.

In order to get more insight on the developing damage, the specimen was scanned by x-ray μCT (Fig. 2c) using a North Star Imaging X25 micro-tomography scanner,

as well. The main adopted parameters consisted in 76 kV voltage, 40 μA amperage, 3 μm focal spot size, magnification equal to 4x and 1200 projections on a 360° rotation of the specimen. A contrast medium was applied in order to enhance the contrast of damage and get a better information.


(a)

(b)

(c)
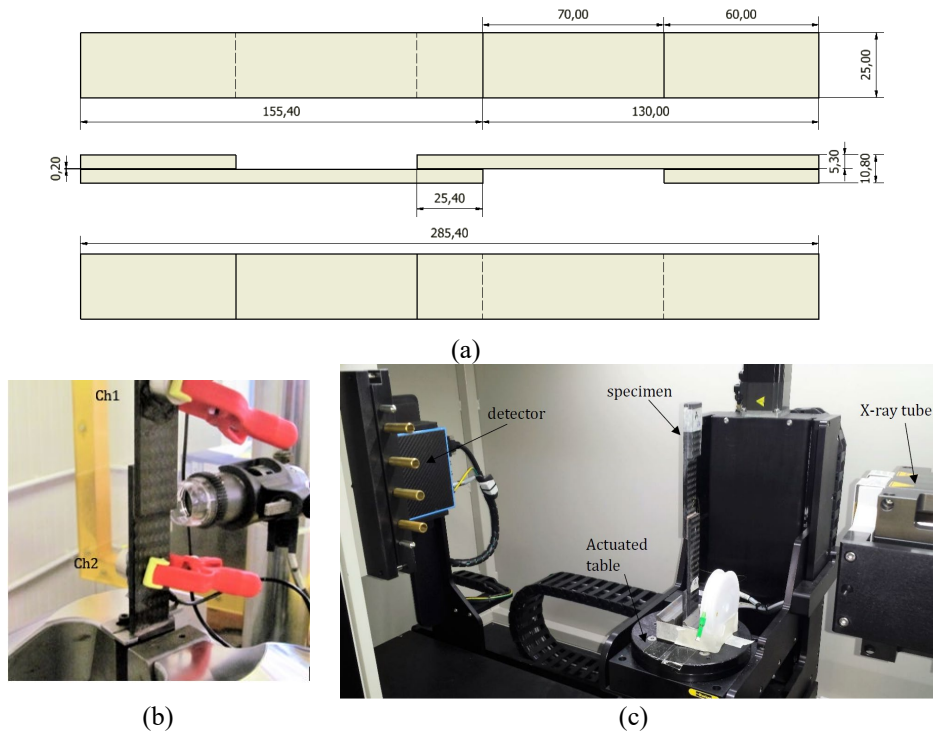
Fig. 2. (a) Specimen adopted for the fatigue test. (b) Set-up for the test, for visual inspections and for structural health monitoring by acoustic emission. (c) Set-up for μCT scans.

SHM by AE was, instead, continuously applied during the test. A Vallen AMSY-6 control unit, equipped with two Vallen VS150-M piezoelectric sensors having frequency range equal to 100-400 kHz with peak frequency equal to 150 kHz (Fig. 2b) and two 34 dB Vallen AEP4 pre-amplifiers, was used. Relevant AE events and their spatial localization, by means of the 1D time of flight triangulation made possible by the two sensors, were acquired. The distance between sensors was equal to 95 mm centered on the overlapped region (Fig. 2b). Sensors were coupled to the specimen by silicon grease and the coupling, along with the performance of the localization, was verified, before the beginning of the test and then periodically, using the standardized "pencil lead break" test by Hsu and Nielsen [10]. The same test allowed determining the sound wave velocity in the specimen, which, on average, resulted to be equal to 3300 m/s. Finally, the control unit was set up to record the displacement of the moving crossbeam of the testing machine, the load signal from the load cell and the number of applied fatigue cycles, as well.

3   Analysis of AE events

Channel 1 recorded 467346 AE events, while channel 2 recorded 615039 events. It is reasonable to expect that just a portion of such acquisitions be related to damage, while the other one can be likely ascribed to background noise. For this reason, in order to have the possibility to evaluate accurately the performance of the proposed AE SHM approach, the recorded AE raw data were classified by a post-processing procedure after the end of the fatigue test. From this point of view, special methods for the classification of sets of numerous objects [11]-[13] are those defined by machine learning and artificial intelligence techniques. For the case at hand, a pattern recognition tool, already successfully applied to another kind of adhesive bonded joint in [14], has been considered. Such a method is based on an unsupervised artificial neural network [15] allowing individuating similar and common features of different objects and makes possible to classify them in homogeneous sets [16].

In detail, the classification procedure starts with the choice of the features to be used to look for similarities between the considered AE events. This was done, in a semi-quantitative way, analyzing many typical features of the recorded AE events by a Multivariate Visual Analysis based on the Parallel Coordinates diagram [6]. The analysis highlighted, as relevant features for the present case, the amplitude, the energy, the rise time, the duration, the counts and the frequency centroid (Fig. 3, [17]). Other considered features did not prove to be significant for the classification of this particular case.
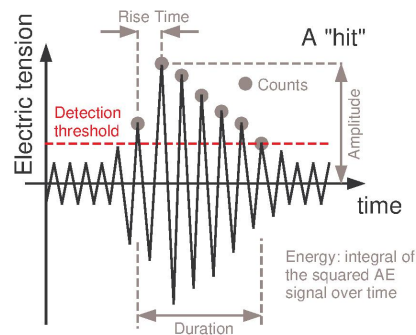

Fig. 3. Scheme of an AE hit (case of burst event) and its relevant features for the present case [17].

After having defined the classifying features, an automatized algorithm, named "k-SOM" and proposed by Crivelli for CFRP composite materials [18], was applied. It is worth remarking that, as each sensor may have a slightly different response, data from channel 1 and 2 were analyzed separately. Nevertheless, k-SOM implements a sequence of steps to analyze the data:

1. a Self-Organizing Map (SOM) [19] in order to get a preliminary indication on how many classes (clusters) the data can be subdivided into. It is an unsuper-

vised algorithm because it is demonstrated [16] that this kind of algorithms is the most appropriate for classifying AE data, whose morphology is typically not known *a priori*;

2. the automatic optimization of the number of classes based on different standardized performance indexes;

3. the conclusive classification by a k-Means algorithm [20].


(a)

(b)
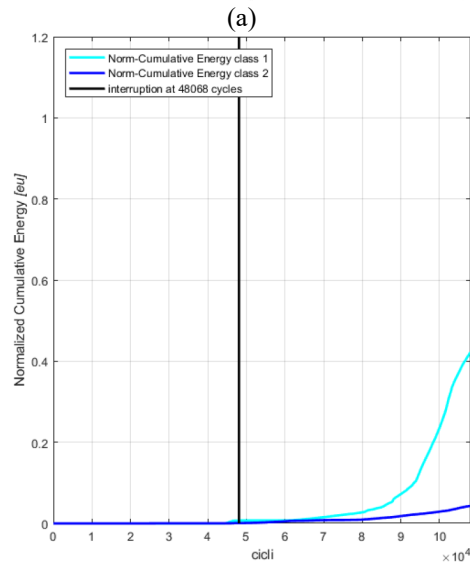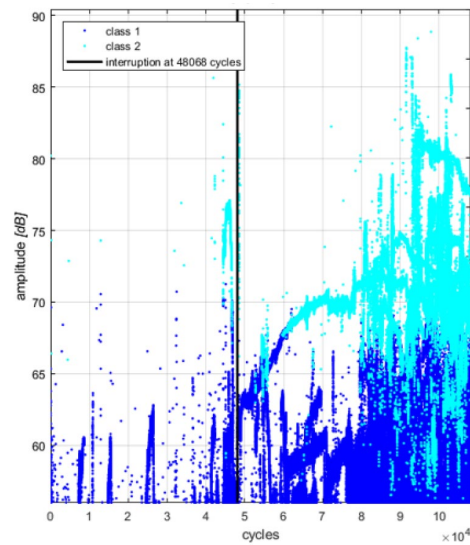
Fig. 4. Trend of classified AE events against the number of fatigue cycles (example of channel 1). (a) Fatigue cycles against amplitude in dB. (b) Fatigue cycles against cumulated energy.

The optimized number of classes, provided by the automatized algorithm, resulted to be two. This could seem in contrast with the abovementioned multiple failure modes of a single lap adhesive bonded joint between CFRP adherends, but, actually, it suggests that, for the case at hand, the waveform of the events related to different failure modes is likely rather similar, even if different from that of noise. A deeper analysis should be carried out in order to classify the different failure modes, but this is beyond the aim of the present research, where the focus is just on detecting damage able to prevent in-service functionality, regardless its type.

The complete set of the classified recorded AE data, for the case of channel 1, is shown in Fig. 4a in terms of amplitude in dB against the number of fatigue cycles, and in Fig. 4b, in terms of cumulated energy against the number of fatigue cycles. Channel 2 showed analogous results. As can be seen, Class 1 is more uniformly distributed in the low-amplitudes region (mean amplitude value equal to 60.3 dB for channel 1 and to 60.2 dB for channel 2) and spans the whole axis of the number of cycles (the typical expected behavior of noise), while Class 2 is more concentrated and variable in the high-amplitudes region (mean amplitude value equal to 71.6 dB for channel 1 and to 74.3 dB for channel 2) and its activity increases with the accumulation of fatigue cycles (the typical expected behavior of fatigue damage). Moreover (Fig. 4b), the cumulated energy of Class 1 shows an almost linear and time-independent trend (typical, again, of noise), while that of Class 2 shows sudden variations of slopes and is time-dependent (typical, again, of damage development). Considering, then, channel 1, 66.6% of AE acquisitions were classified into Class 1, while the remaining 33.4% into Class 2. Likewise, for channel 2, 69.8% of AE acquisitions were classified into Class 1, while the remaining 30.2% into Class 2.

A further simple check consisted in the visual analysis of the morphology of the waveforms included into the defined classes. Fig. 5 shows some emblematic examples: Class 1 includes the typical waveforms related to background noise, while Class 2 those related to damage phenomena (particularly, fracture).


(a)   (b)
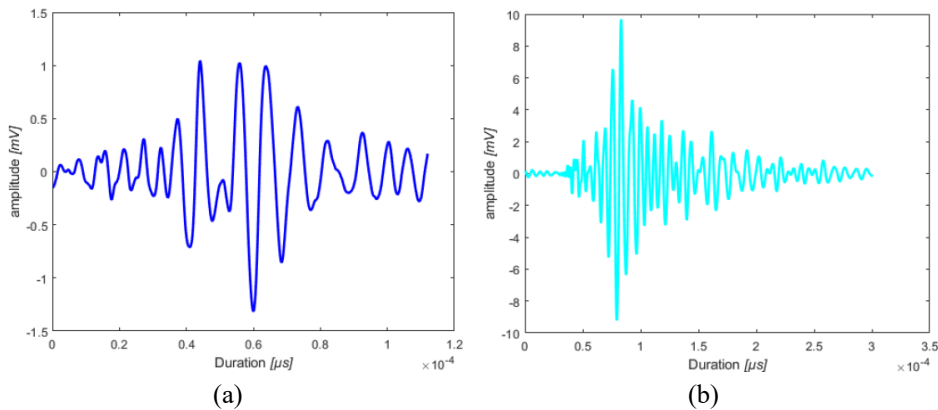
Fig. 5. Typical waveforms included into the two classes. (a) Class 1. (b) Class 2.

8

A final validation of this conclusion and of the proposed SHM approach is the comparison to the results obtained by the NDT techniques applied during the fatigue test. Particularly, in order to check if the proposed SHM approach is able to detect the first stages of damage development, the fatigue test was interrupted, for the first time, at 49100 cycles, i.e. just after the first AE events classified in Class 2 were observed (Fig. 4a). Fig. 6 shows the results of visual testing applied at the edges of the over-lapped region of the adherends after 49100 fatigue cycles. As can be seen, the upper edge presents the initiation of micro-cracks which were not detected by the same in-spection carried out at 0 fatigue cycles, while the lower edge was still intact. This is confirmed by the µCT analysis of the overlapped region of the adherends after 49100 fatigue cycles (Fig. 7) and suggests that, actually, the first recorded AE events classi-fied in Class 2 could be due to the initiation of fatigue cracks in the specimen.
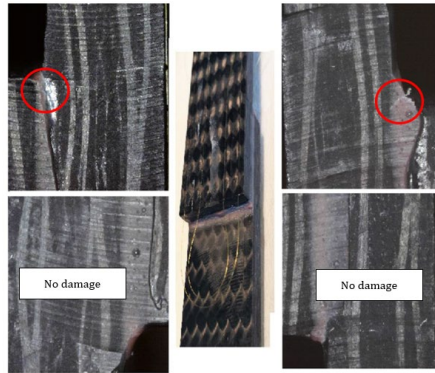
Fig. 6. Visual testing of the edges of the overlapped region of the adherends after 49100 fatigue cycles.

(a)   (b)
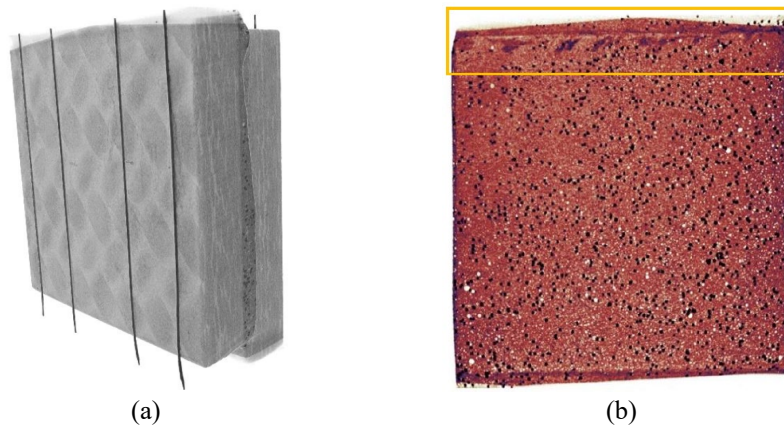
Fig. 7. µCT analysis of the overlapped region of the adherends after 49100 fatigue cycles. (a) Region of interest. (b) Slice of the fatigue damaged region (false colors).

4   Localization of AE events

A very fast release of elastic energy in the material, e.g. in the case of an advancing crack, generates an AE event in the form of an elastic wave that propagates in all directions. Depending on the position of the source, the released wave reaches the applied sensors with given, and generally different, delays (times of flight) [7]. Assuming the considered lap joint as a one-dimensional linear system, two sensors are enough and, consequently, localization was applied with two aims:

1. as a further check of the effectiveness of the classification algorithm;
2. to check the ability of the proposed SHM approach to localize the developing fatigue damage, i.e. the AE source, in the considered lap joint configuration.

The analysis was carried out considering just the AE events classified in Class 2, i.e. the one here assumed to be related to the developing fatigue damage. Fig. 8 shows, then, the energy distribution of the localized events as a function of the position along the specimen. As can be seen, the cumulative energy, i.e. the most energetic AE events, tended to gather in correspondence of the overlap ends, where damage initiated and propagated, as observed by VT and μCT. In particular, most of the energy was released at the overlap end close to channel 2, i.e. the one presenting, at the end of the fatigue test, the highest AE activity. It can be concluded that localization furtherly validates the proposed classification algorithm and proves to be effective in the perspective of in-field SHM application to the considered kind of lap-joints.
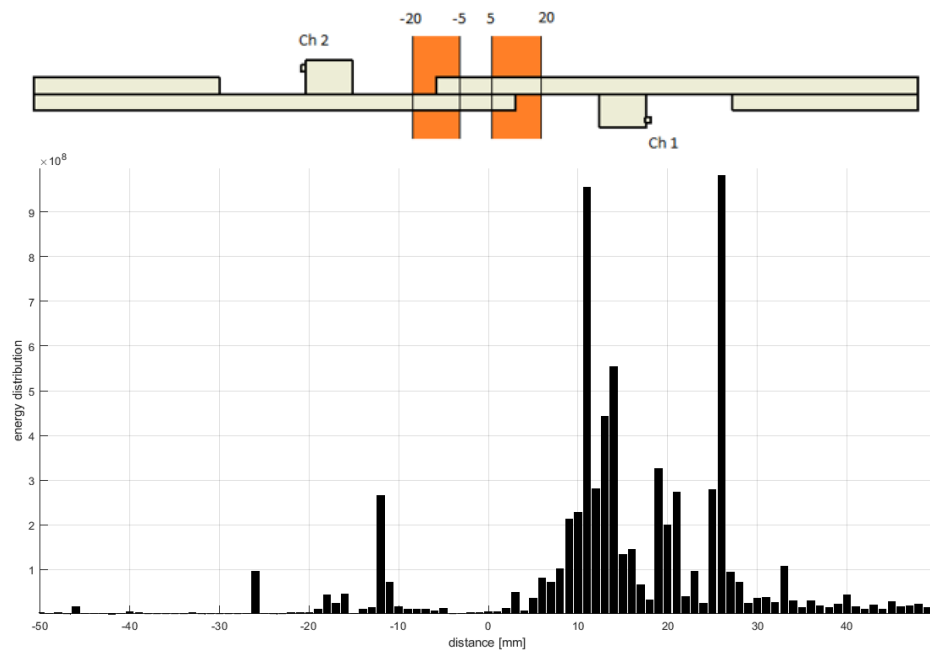

Fig. 8. Localization of AE events.

5   Concluding remarks

The performance of a structural health monitoring approach, based on acoustic emission, was evaluated considering the applicative case of a single lap CFRP-CFRP adhesive bonded joint subjected to fatigue loading. Damage development was, also, investigated by visual testing and x-ray micro-computed tomography, which fully validated the proposed monitoring method. Results showed that monitoring by acoustic emission, after the application of suitable pattern recognition algorithms, allows detecting, in adhesive bonded joints of CFRP adherends, the early initiation of fatigue cracks in an effective way and that the application of localization of AE sources can be an effective help to interpret the developing damage.

Acknowledgements

References

[1] Banea, M.D., Da Silva, L.F.M.: Adhesively bonded joints in composite materials: an overview. Proceedings of the Institution of Mechanical Engineers, Part L, Journal of Materials: Design and Applications 223(1), 1-18 (2009).

[2] ASTM D 5573-99: Standard practice for classifying failure modes in fibre-reinforced-plastic (FRP) joints. Annual Book of ASTM Standards (2002).

[3] Adams, R.D., Cawley, P.: A review of defect types and non-destructive testing techniques for composites and bonded joints. NDT International 21(4), 208-222 (1988).

[4] Adams, R.D., Drinkwater, B.W.: Non–destructive testing of adhesively bonded joints. International Journal of Materials and Product Technology 14(5-6), 385-398 (1999).

[5] Chang, F.K.: Introduction to health monitoring, context, problems, solutions. Presentation at the first European Pre-workshop on Structural Health Monitoring, Paris, France (2009).

[6] Carmignato, S., Dewulf, W., Leach, R.: Industrial X-ray computed tomography. Springer, Berlin Heidelberg (2018).

[7] Grosse, C.U., Ohtsu, M.: Acoustic Emission Testing. Springer, Berlin Heidelberg (2008).

[8] Bernasconi, A., Carboni, M., Comolli, L., Galeazzi, R., Gianneo, A., Kharshiduzzaman, M.: Fatigue crack growth monitoring in composite bonded lap joints by a distributed fibre optic sensing system and comparison with ultrasonic testing. The Journal of Adhesion 92(7-9), 739-757 (2016).

[9] Gianneo, A., Carboni, M., Bernasconi A.: Crack Profile Reconstruction of CFRP-CFRP Bonded Joints from Optical Backscatter Reflectometry and Comparison with X-ray Computed Tomography. In: 14th International Conference of the Slovenian Society for Non-Destructive Testing "Application of Contemporary Non-Destructive Testing in Engineering". Portorož, Slovenia (2017).

[10] ASTM E 976-15: Standard Guide for Determining the Reproducibility of Acoustic Emission Sensor Response. ASTM International, West Conshohocken, Pennsylvania (2015).

[11] Batchelor, B.G.: Practical approach to pattern classification. Plenum Press, New York (1974).

[12] Jain, A.K., Murty, M.N., Flynn, P.J.: Data clustering: a review. ACM Computing Surveys (CSUR) 31(3), 264-323 (1999).

[13] Haykin, S.: Neural Networks and Learning Machines. 3rd edition, Pearson Education Inc., Upper Saddle River, New Jersey, USA (2009).

[14] Carboni, M., Bernasconi, A.: Application of Acoustic Emission for Monitoring Fatigue Damage in CFRP-CFRP Adhesive Bonded Joints. Proc. 15th International Symposium on Nondestructive Characterization of Materials, Portorož, Slovenia (2019).

[15] Miller, R.K., Hill, E.v.K., Moore P.O.: Acoustic Emission Testing". In Nondestructive Testing Handbook, vol. 6, 3rd edition, American Society for Nondestructive Testing, Columbus, Ohio, USA (2005).

[16] Batchelor, B.G.: Pattern recognition: ideas in practice. Springer Science & Business Media, Berlin Heidelberg (2012).

[17] Carboni, M., Crivelli, D.: An acoustic emission based structural health monitoring approach to damage development in solid railway axles. International Journal of Fatigue 139, 105753 (2020).

[18] Crivelli, D.: Structural health monitoring with acoustic emission and neural networks. Ph.D. thesis, Politecnico di Milano, Italy (2014).

[19] Miljković, D.: Brief review of self-organizing maps. 40th International Convention on Information and Communication Technology, Electronics and Microelectronics (MIPRO), Opotija, Croatia (2017).

[20] Krishna, K., Murty, M.N.: Genetic K-means algorithm. IEEE Transactions on Systems, Man, and Cybernetics, Part B (Cybernetics) 29(3), 433-439 (1999).